

Space matters: Li⁺ conduction versus strain effect at FePO₄/LiFePO₄ interface

Weiqliang Lv, Yinghua Niu, Xian Jian, Kelvin H. L. Zhang, Wei Wang, Jiyun Zhao, Zhiming Wang, Weiqliang Yang, and Weidong He'

Citation: *Appl. Phys. Lett.* **108**, 083901 (2016); doi: 10.1063/1.4942849

View online: <http://dx.doi.org/10.1063/1.4942849>

View Table of Contents: <http://aip.scitation.org/toc/apl/108/8>

Published by the [American Institute of Physics](#)



**FIND THE NEEDLE IN THE
HIRING HAYSTACK**

POST JOBS AND REACH THOUSANDS OF
QUALIFIED SCIENTISTS EACH MONTH.

PHYSICS TODAY | JOBS
WWW.PHYSICSTODAY.ORG/JOBS

Space matters: Li^+ conduction versus strain effect at $\text{FePO}_4/\text{LiFePO}_4$ interface

Weiqliang Lv,¹ Yinghua Niu,¹ Xian Jian,¹ Kelvin H. L. Zhang,² Wei Wang,³ Jiyun Zhao,⁴ Zhiming Wang,⁵ Weiqing Yang,⁶ and Weidong He^{1,a)}

¹School of Energy Science and Engineering, University of Electronic Science and Technology, Chengdu 611731, People's Republic of China

²Department of Materials Science and Metallurgy, University of Cambridge, 27 Charles Babbage Road, Cambridge CB3 0FS, United Kingdom

³School of Materials Science and Engineering, Shenzhen Graduate School, Harbin Institute of Technology, Shenzhen 518055, People's Republic of China

⁴Department of Mechanical and Biomedical Engineering, City University of Hong Kong, Kowloon, Hong Kong

⁵Institute of Fundamental and Frontier Sciences, University of Electronic Science and Technology of China, Chengdu 610054, People's Republic of China

⁶Key Laboratory of Advanced Technologies of Materials (Ministry of Education), School of Materials Science and Engineering, Southwest Jiaotong University, Chengdu 610031, People's Republic of China

(Received 14 December 2015; accepted 15 February 2016; published online 25 February 2016)

$\text{FePO}_4/\text{LiFePO}_4$ (FP/LFP) interfacial strain, giving rise to substantial variation in interfacial energy and lattice volume, is inevitable in the (de)lithiation process of LiFePO_4 , a prototype of Li ion battery cathodes. Extensive theoretical and experimental research has been focused on the effect of lattice strain energy on FP/LFP interface propagation orientation and cyclic stability of the electrode. However, the essential effect of strain induced lattice distortion on Li^+ transport at the FP/LFP interface is typically overlooked. In this report, a coherent interface model is derived to evaluate quantitatively the correlation between FP/LFP lattice distortion and Li^+ conduction. The results illustrate that the effect of lattice strain on Li^+ conduction depends strongly on FP/LFP interface orientations. Lattice strain induces a 90% decrease of Li^+ conductivity in *ac*-plane oriented (de)lithiation at room temperature. The opposite effect of lattice strain on delithiation and lithiation for *ab*- and *bc*-orientations is elucidated. In addition, the effect of lattice strain tends to be more pronounced at a lower working temperature. This study provides an efficient platform to comprehend and manipulate Li^+ conduction in the charge and discharge of lithium ion batteries, the large-scale application of which is frequently challenged by limited in-cell ion conduction.

© 2016 AIP Publishing LLC. [<http://dx.doi.org/10.1063/1.4942849>]

LiFePO_4 (LFP) is a commercialized cathode material employed frequently in electrical vehicle (EV) batteries due to its high safety, long cyclic life, and low cost.¹ However, the material is still subject to insightful study for improvement in its capacity and rate performance.² For instance, carbon coating strategy has been employed to improve the poor intrinsic electronic conductivity, and particle size reduction and aliovalent doping have been adopted to enhance the Li^+ conductivity.^{3–5} Compared to the electronic conduction, the low Li^+ conductivity is still the limiting factor for the fast kinetics of charge/discharge process.^{2,6,7} The rather limited Li solubility in LiFePO_4 and FePO_4 (FP) suggests that (de)lithiation in this material proceeds with a two-phase mechanism, where the relative $\text{LiFePO}_4:\text{FePO}_4$ phase ratio varies with moving phase boundary, as first proposed by Padhi *et al.*,¹ and elucidated further by subsequent experimental observations.^{8,9} The delithiated phase FePO_4 has essentially the same structure as LiFePO_4 , yet with a $\sim 6\%$ reduction in cell volume. Such a lattice mismatch causes interfacial strain, which impacts largely the electrochemical performance in the battery (de)lithiation of LiFePO_4 as cathode. Van

der Ven *et al.* have illustrated the effect of coherency strains on the thermodynamics of two-phase coexistence and the voltage profile during Li (de)intercalation of LiFePO_4 .¹⁰ Tang *et al.* have revealed that the misfit strain energy has a considerable influence on FP/LFP phase transformation orientation and morphology.¹¹ Through analysis of interfacial energy and coherency strain energy, Abdellahi *et al.* have shown that the preferred interface orientation for FP/LFP phase transformation is dependent on both particle size and particle morphology.¹² Despite the aforementioned studies, quantitative investigation into the effect of FP/LFP interfacial strain induced lattice cell volume variation (ΔV) on Li^+ transport at FP/LFP interface is still lacking. In this study, FP/LFP interfacial strain arising from the lattice mismatch is investigated by building a coherent interface elastic model. The quantitative correlations between lattice strain and lattice cell volume variation and between the lattice cell volume variation and the activation energy change of Li^+ transport (ΔG) are both illustrated. Temperature effect on strain induced Li^+ transport is also given. Our work provides a model to understand the Li^+ transport in LiFePO_4 and other two-phase electrode materials for lithium ion batteries (LIBs), and facilitates the optimization of LIBs with superior rate performance.

^{a)} Author to whom correspondence should be addressed. Electronic mail: weidong.he@uestc.edu.cn

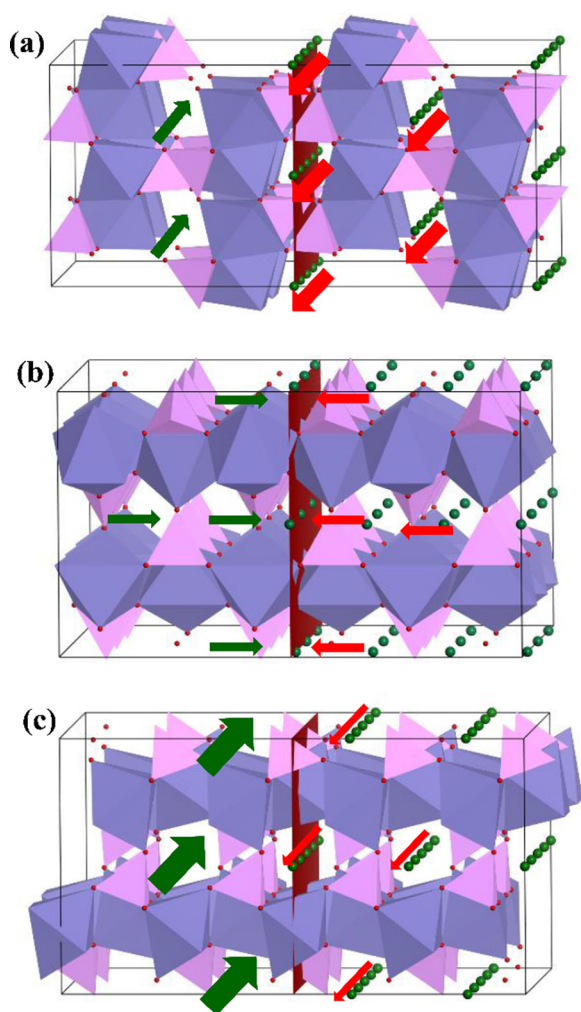


FIG. 1. Atomic models of $\text{FePO}_4/\text{LiFePO}_4$ interfaces along (a) bc plane, (b) ac plane, and (c) ab plane. The green atoms denote Li, the pink tetrahedra stand for PO_4 structure and the octahedra stand for FeO_6 structure. The brown planes stand for FP/LFP interfaces. The red arrows show delithiation (charge) [010] direction, whereas the green arrows show lithiation (discharge) [010] direction.

The propagation of FP/LFP interface through bc plane,^{13–15} ac ,^{16,17} and ab ¹⁸ planes is all observed experimentally. At the cathode, LiFePO_4 particles of various sizes and shapes form three dimensional Li^+ conductive cross-linked network. The (de)lithiation can proceed along a number of interface orientations including bc , ac , and ab planes among others, as given in Fig. 1. Evaluation on the correlation between the orientations of the FP/LFP interface and Li^+ diffusion is thus critical for understanding the effect of

interfacial strain on Li^+ conduction. Due to the anisotropy of Li^+ diffusion preferable along [010] direction,^{19–21} Li^+ diffusion paths at typical bc -, ac -, and ab -FP/LFP interfaces are demarked by red arrows for the delithiation path in the LFP phase and green arrows for the lithiation path in the FP phase. As shown in Fig. 1, Li^+ diffuses along bc and ab interfaces in bc - and ab -oriented (de)lithiation, and diffuses across the ac interface for ac -oriented (de)lithiation. For bc - and ab -oriented two-phase transformation, the charge rate is dependent on the delithiation in LFP phase, whereas the discharge rate is dependent on the lithiation in FP phase. The (de)lithiation rate for ac -oriented two-phase transformation is dependent on Li^+ conductivities of both FePO_4 and LiFePO_4 and limited by the smaller one.

A coherent FP/LFP interface model with lattice mismatch, as shown in Fig. 2(a), is built to evaluate the lattice strain and cell volume change. The detailed derivation is depicted in the supplementary material.²² The crystallographic orientation dependent FP/LFP interfacial strain and cell volume change are calculated with lattice constants²³ and elastic constants²⁴ of FePO_4 and LiFePO_4 , as shown in Table S1 in the supplementary material. ΔG is derived from the plot of ΔG versus $\Delta V/V$ based on available density functional theory (DFT) data.²⁵ As shown in Fig. 2(b), ΔG exhibits a quasi-linear correlation with $\Delta V/V$ as the cell volume varies in the range of $\pm 6\%$. The slope of ΔG versus $\Delta V/V$ is ~ -0.015 eV, depending on the physical nature of LiFePO_4 , including the cell structure, the elastic modulus, and other parameters impacting the interaction between transporting Li^+ and the surrounding atoms in LiFePO_4 . ΔV and ΔG with respect to a specific interface exhibit opposite values for LFP and FP phases, indicating that FP/LFP interfacial strain has opposite impact on the delithiation of LFP phase and lithiation of FP phase. ΔG with respect to the ab interface for each phase is the largest, followed by those with respect to the ac interface and the bc interface. LFP cell volume at the bc interface increases 1.57%, and ΔG decreases 0.025 eV accordingly. The LFP phase at the ab and ac interfaces experiences compressive strain and increased ΔG of Li^+ transport. The cell volumes of FP at ac and ab interfaces expand $\sim 3.51\%$ and 5.04% , resulting in decreased ΔG of 0.058 eV and 0.075 eV, respectively. The cell volume of FP at the bc interface (FP(bc)) is compressed $\sim 1.55\%$, resulting in an increased ΔG of 0.025 eV.

The Li^+ conductivity at strained interface (σ_i) is correlated to bulk conductivity (σ_0) by Eq. (S12) in the supplementary material.²² As shown in Fig. 3, $\lg \frac{\sigma_i}{\sigma_0}$ for LFP and FP

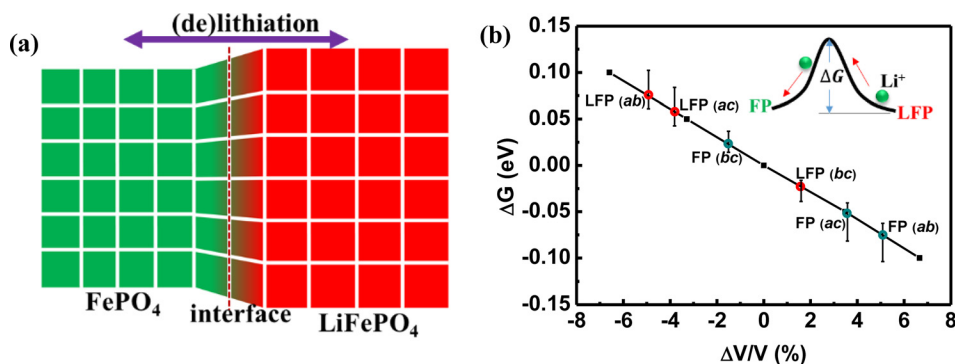


FIG. 2. (a) Schematics of coherent interfaces with lattice mismatch. (b) The plot of activation energy variation of Li^+ transport as a function of strain-induced lattice cell volume change. The black square dots represent DFT data from Ref. 24. The red (green) circles denote data points of ($\Delta V/V$, ΔG) with error bars for LiFePO_4 (FePO_4) with a specific interface orientation. LFP(ab) stands for the LFP phase at the ab interface.

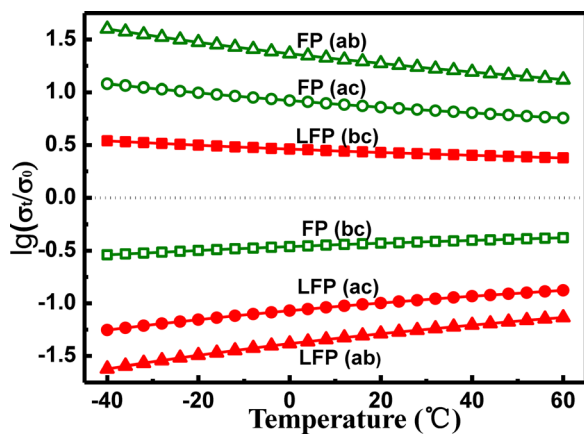


FIG. 3. Temperature dependence of interfacial strain induced Li^+ conductivity variation of FePO_4 and LiFePO_4 .

phases along a specific interface orientation is in value. For instance, at 25°C , $\lg \frac{\sigma_t}{\sigma_0}$ is 1.26 for $\text{FP}(ab)$ and is -1.27 for $\text{LFP}(ab)$, indicating that the delithiation Li^+ conductivity decreases to only $\sim 0.05 \sigma_0$ and the lithiation Li^+ conductivity increases to $\sim 18 \sigma_0$. For $\text{FP}(bc)$ and $\text{LFP}(bc)$, $\lg \frac{\sigma_t}{\sigma_0}$ is -0.42 and 0.42 , respectively. The result suggests that the bc -delithiation Li^+ conductivity increases to $\sim 2.66 \sigma_0$, whereas the bc -lithiation Li^+ conductivity decreases to $0.38 \sigma_0$ at room temperature. $\lg \frac{\sigma_t}{\sigma_0}$ for $\text{FP}(ac)$ and $\text{LFP}(ac)$ is 0.85 and -0.98 , respectively, but the Li^+ conduction for the lithiation and delithiation is dependent on the smaller σ_t of $\sim 0.10 \sigma_0$ at room temperature since Li^+ diffuses across the ac interface. It is proposed that the (de)lithiation in the cathode composed of LiFePO_4 particles occurs along multiple interface orientations. Depending upon the specific interface orientation, interfacial strain induces 1–2 folds of impact on Li^+ conductivity. Such diverse strain effects explain, to a rational extent, the known inconsistency between the Li^+ conductivity of $\sim 10^{-8} \text{cm}^2/\text{s}$ by DFT/molecular dynamics (MD) and the experimental value of $\sim 10^{-10} \text{cm}^2/\text{s}$ at room temperature.^{7,19,20,26}

The Li^+ conduction of the LFP cathode is limited largely at a low temperature or an essentially elevated temperature.^{27,28} As shown in Fig. 3, the absolute value $|\lg \frac{\sigma_t}{\sigma_0}|$ increases for both FP and LFP phases of all three interface orientations as temperature decreases, indicating that the interfacial strain has more profound impact on Li^+ conductivity at a lower temperature. For instance, $\lg \frac{\sigma_t}{\sigma_0}$ along $\text{FP}(ab)$ increases from 1.12 to 1.60, and $\lg \frac{\sigma_t}{\sigma_0}$ along $\text{LFP}(bc)$ increases from 0.38 to 0.54 as the temperature decreases from 60°C to -40°C . It should be noted that σ_0 typically decreases exponentially as temperature decreases, and, thus, the overall charge/discharge rate still decreases as temperature decreases. Nevertheless, FP/LFP interfacial strain can be utilized to enhance the low-temperature Li^+ conduction. For instance, interfacial strain improves notably the lithiation Li^+ conduction for $\text{FP}(ab)$ and the delithiation Li^+ conduction for $\text{LFP}(bc)$ according to our results.

It should be noted the two-phase interface should be sharp, and the deviation from the sharp interface in the analysis influences largely the values of lattice strain and activation energy of Li^+ conduction.²⁹ Experimental evidences for the anisotropy of the FP/LFP interface propagation are yet inadequate at this moment since the phase transformation is

correlated with lattice defects,³⁰ surface states,³¹ and particle micro-structure.³² Undoubtedly, *in-situ* characterizations and atomic-scale simulations at single-particle scale will facilitate future investigations into the FP/LFP interface propagation kinetics.

In summary, the FP/LFP interfacial strain induced lattice cell volume as well as the activation energy of Li^+ transport is investigated. The Li^+ conductivity of LFP is affected largely by the two-phase interfacial strain. At room temperature, Li^+ conductivity at the ac -oriented FP/LFP interface decreases to $\sim 10\%$ of the bulk value. Li^+ conductivity at the bc interface experiences the smallest impact of interfacial strain, and exhibits a 166% increase in delithiation and a 62% decrease in lithiation. Such a lattice strain effect is more pronounced at a lower working temperature.

The work was supported by UESTC new faculty startup fund, the National Natural Science Foundation (Grant Nos. 21403031 and 51501030) and the Fundamental Research Funds for the Chinese Central Universities (Grant No. ZYGX2014J088).

¹A. K. Padhi, K. S. Nanjundaswamy, and J. B. Goodenough, "Phospho-olivines as positive-electrode materials for rechargeable lithium batteries," *J. Electrochem. Soc.* **144**(4), 1188 (1997).

²J. Wang and X. Sun, "Olivine LiFePO_4 : The remaining challenges for future energy storage," *Energy Environ. Sci.* **8**(4), 1110–1138 (2015).

³J. Wang and X. Sun, "Understanding and recent development of carbon coating on LiFePO_4 cathode materials for lithium-ion batteries," *Energy Environ. Sci.* **5**(1), 5163–5185 (2012).

⁴W. J. Zhang, "Comparison of the rate capacities of LiFePO_4 cathode materials," *J. Electrochem. Soc.* **157**(10), A1040–A6 (2010).

⁵R. Malik, D. Burch, M. Bazant, and G. Ceder, "Particle size dependence of the ionic diffusivity," *Nano Lett.* **10**(10), 4123–4127 (2010).

⁶M. Park, X. Zhang, M. Chung, G. B. Less, and A. M. Sastry, "A review of conduction phenomena in Li-ion batteries," *J. Power Sources* **195**(24), 7904–29 (2010).

⁷R. Malik, A. Abdellahi, and G. Ceder, "A critical review of the Li insertion mechanisms in LiFePO_4 electrodes," *J. Electrochem. Soc.* **160**(5), A3179–A3197 (2013).

⁸C. V. Ramana, A. Mauger, F. Gendron, C. M. Julien, and K. Zaghib, "Study of the Li-insertion/extraction process in $\text{LiFePO}_4/\text{FePO}_4$," *J. Power Sources* **187**(2), 555–64 (2009).

⁹C. T. Love, A. Korovina, C. J. Patridge, K. E. Swider-Lyons, M. E. Twigg, and D. E. Ramaker, "Review of LiFePO_4 phase transition mechanisms and new observations from X-ray absorption spectroscopy," *J. Electrochem. Soc.* **160**(5), A3153–A61 (2013).

¹⁰A. Van der Ven, K. Garikipati, S. Kim, and M. Wagemaker, "The role of coherency strains on phase stability in Li_xFePO_4 : Needle crystallites minimize coherency strain and overpotential," *J. Electrochem. Soc.* **156**(11), A949–A957 (2009).

¹¹M. Tang, J. F. Belak, and M. R. Dorr, "Anisotropic phase boundary morphology in nanoscale olivine electrode particles," *J. Phys. Chem. C.* **115**(11), 4922–4926 (2011).

¹²A. Abdellahi, O. Akyildiz, R. Malik, K. Thornton, and G. Ceder, "Particle-size and morphology dependence of the preferred interface orientation in LiFePO_4 nano-particles," *J. Mater. Chem. A* **2**(37), 15437–15447 (2014).

¹³G. Chen, X. Song, and T. J. Richardson, "Electron microscopy study of the LiFePO_4 to FePO_4 phase transition," *Electrochem. Solid-State Lett.* **9**(6), A295–A298 (2006).

¹⁴C. Delmas, M. Maccario, L. Croguennec, F. Le Cras, and F. Weill, "Lithium deintercalation in LiFePO_4 nanoparticles via a domino-cascade model," *Nat. Mater.* **7**(8), 665–671 (2008).

¹⁵P. Bai, D. A. Cogswell, and M. Z. Bazant, "Suppression of phase separation in LiFePO_4 nanoparticles during battery discharge," *Nano Lett.* **11**(11), 4890–4896 (2011).

¹⁶S. Park, C. Park, J. Hwang, W. Cho, and H. Jang, "Anisotropic lithium ion migration in LiFePO_4 ," *Met. Mater. Int.* **17**(6), 1017–1720 (2011).

- ¹⁷H. Gabrisch, J. Wilcox, and M. Doeff, "TEM study of fracturing in spherical and plate-like LiFePO₄ particles," *Electrochem. Solid-State Lett.* **11**(3), A25–A29 (2008).
- ¹⁸L. Suo, W. Han, X. Lu, L. Gu, Y. S. Hu, H. Li, D. F. Chen, L. Q. Chen, S. Tsukimoto, and Y. Ikuhara, "Highly ordered staging structural interface between LiFePO₄ and FePO₄," *Phys. Chem. Chem. Phys.* **14**(16), 5363–5367 (2012).
- ¹⁹M. S. Islam, D. J. Driscoll, C. A. J. Fisher, and P. R. Slater, "Atomic-scale investigation of defects, dopants, and lithium transport in the LiFePO₄ olivine-type battery material," *Chem. Mater.* **17**(20), 5085–5092 (2005).
- ²⁰D. Morgan, A. Van der Ven, and G. Ceder, "Li conductivity in Li_xMPO₄ (M = Mn, Fe, Co, Ni) olivine materials," *Electrochem. Solid-State Lett.* **7**(2), A30–A32 (2004).
- ²¹S. i. Nishimura, G. Kobayashi, K. Ohoyama, R. Kanno, M. Yashima, and A. Yamada, "Experimental visualization of lithium diffusion in Li_xFePO₄," *Nat. Mater.* **7**, 707–711 (2008).
- ²²See supplementary material at <http://dx.doi.org/10.1063/1.4942849> for the detailed derivation of FePO₄/LiFePO₄ interfacial orientation dependent strains and the calculation parameters.
- ²³G. Rouse, J. Rodriguez-Carvajal, S. Patoux, and C. Masquelier, "Magnetic structures of the triphylite LiFePO₄ and of its delithiated form FePO₄," *Chem. Mater.* **15**(21), 4082–4090 (2003).
- ²⁴T. Maxisch and G. Ceder, "Elastic properties of olivine Li_xFePO₄ from first principles," *Phys. Rev. B* **73**(17), 174112 (2006).
- ²⁵J. Lee, S. J. Pennycook, and S. T. Pantelides, "Simultaneous enhancement of electronic and Li⁺ ion conductivity in LiFePO₄," *Appl. Phys. Lett.* **101**(3), 033901 (2012).
- ²⁶J. Sugiyama, H. Nozaki, M. Harada, K. Kamazawa, O. Ofer, M. Månsson, J. H. Brewer, E. J. Ansaldo, K. H. Chow, Y. Ikeda *et al.*, "Magnetic and diffusive nature of LiFePO₄ investigated by muon spin rotation and relaxation," *Phys. Rev. B* **84**, 054430 (2011).
- ²⁷G. Zhu, K. Wen, W. Lv, X. Zhou, Y. Liang, F. Yang, Z. Chen, M. Zou, J. Li, Y. Zhang *et al.*, "Materials insights into low-temperature performances of lithium-ion batteries," *J. Power Source* **300**, 29–40 (2015).
- ²⁸Y. Liang, K. Wen, Y. Mao, Z. Liu, G. Zhu, F. Yang, and W. He, "Shape and size control of LiFePO₄ for high-performance lithium-ion batteries," *ChemElectroChem* **2**(9), 1227–1237 (2015).
- ²⁹G. Kobayashi, S. Nishimura, M. S. Park, R. Kanno, M. Yashima, T. Ida, and A. Yamada, "Isolation of solid solution phases in size-controlled Li_xFePO₄ at room temperature," *Adv. Funct. Mater.* **19**(3), 395–403 (2009).
- ³⁰S. Y. Chung, S. Y. Choi, T. Yamamoto, and Y. Ikuhara, "Atomic-scale visualization of antisite defects in LiFePO₄," *Phys. Rev. Lett.* **100**(12), 125502 (2008).
- ³¹B. Kang and G. Ceder, "Battery materials for ultrafast charging and discharging," *Nature* **458**(7235), 190–193 (2009).
- ³²Y. Zhao, L. Peng, B. Liu, and G. Yu, "Single-crystalline LiFePO₄ nanosheets for high-rate Li-Ion batteries," *Nano Lett.* **14**(5), 2849–2853 (2014).